DOI: 10.61782/fa.2023.1191

CONSIDERATIONS FOR MASS-SPRING POROUS ABSORBER CHARACTERIZATION APPROACHES BASED ON FINITE ELEMENT MODELLING

Mariia Bronzova[1,2*] **Arnaud Bocquillet**[1] **Martin Schanz**[2]
[1] Passenger Compartment, Aero Acoustics Department, BMW AG, Munich, Germany
[2] Institute of Applied Mechanics, Graz University of Technology, Austria

ABSTRACT

Structure-borne sound protection is one of the vital aspects when it comes to the topic of vehicle acoustics. Mass-spring systems are actively used to absorb vibroacoustic energy and thus to reduce the overall noise level inside a car cabin. A precise material parameter definition of the foam part of a mass-spring system is imperative for accurate numerical simulation results. However, traditional material characterization approaches often rely on measurement data acquired for setups that modify porous layer material properties, for instance, due to pre-stressing conditions or the influence of interface effects between the absorber and excitation structure. This paper presents a new approach to obtain realistic absorber material parameters by the means of inverse problem optimization techniques in the framework of Finite Element Modelling (FEM).

Keywords: *Porous absorber, mass-spring systems, numerical simulation, acoustics.*

1. INTRODUCTION

In the last decades the topic of the vehicle acoustic comfort has come to the forefront as one of the major factors influencing customer automobile preferences [1]. Car body vibrations together with the accompanying noise do not only reduce acoustic comfort, but also cause driver fatigue. As a result, driving safety reduces, which increases the importance of the topic of noise and vibration damping techniques [2]. Commonly trim interior materials are used for sound-absorbing purposes inside vehicles [3]. In particular mass-spring systems consisting of poroelastic foams casted together with an elastic heavy layer on top increase sound transmission losses [4].
For the description of sound propagation within coupled materials made of solid matrix and fluid the Biot poroelasticity theory [5–7] is typically used. Having accounted for the inertial interaction between the frame and the fluid of the foam, Biot introduced a profound model expressing acoustic wave propagation as of two compressional and one shear waves [8]. The mixed displacement-pressure $(\mathbf{u}^s, p)$ formulation (three displacements of the solid phase and the interstitial pressure of the fluid phase) of the Biot theory [9, 10] is often preferred, as it is considered more computationally efficient than the alternative $(\mathbf{u},\mathbf{U})$ displacement formulation with three solid and three pore-fluid displacements respectively [11]. Besides, in the weak integral form the coupling between two phases occurs naturally, thus, making the $(\mathbf{u}^s, p)$ Biot formulation even more efficacious. The discretized form of the weak integral Biot equations [8] was implemented in this paper for numerical studies:

$$\begin{bmatrix} [\mathbf{Z}] & -[\tilde{\mathbf{C}}] \\ -[\tilde{\mathbf{C}}]^\intercal & [\mathbf{A}] \end{bmatrix} \begin{Bmatrix} \mathbf{u}^\mathrm{s} \\ \mathbf{p} \end{Bmatrix} = \begin{Bmatrix} \mathbf{F}^\mathrm{s} \\ \mathbf{F}^\mathrm{f} \end{Bmatrix}, \tag{1}$$

where $\mathbf{u}^\mathrm{s}$ and $\mathbf{p}$ are solid and fluid phase nodal values. $[\mathbf{Z}] = -\omega^2[\tilde{\mathbf{M}}] + [\tilde{\mathbf{K}}]$ is the mechanical impedance matrix of the skeleton with equivalent mass $[\tilde{\mathbf{M}}]$ and stiffness

**Corresponding author*: *Mariia.MB.Bronzova@bmw.de.*

$[\tilde{\mathbf{K}}]$ matrices. $[\mathbf{A}] = [\tilde{\mathbf{H}}]/\omega^2 - [\tilde{\mathbf{Q}}]$ is the acoustic admittance matrix of the interstitial fluid with $[\tilde{\mathbf{H}}]$ and $[\tilde{\mathbf{Q}}]$ being equivalent kinetic and compression energy matrices of the fluid phase. $[\tilde{\mathbf{C}}] = [\tilde{\mathbf{C_1}}] + [\tilde{\mathbf{C_2}}]$ is the volume coupling matrix between the skeleton and fluid variables. $\mathbf{F^s}$ is the surface load vector for the skeleton and $\mathbf{F^f}$ is the surface kinematic coupling vector for the fluid.
A number of porous absorber parameters are hidden inside the matrices above. Thus, Young's modulus of the skeleton together with the loss factor and Poisson's ratio are necessary to establish the stiffness matrix:

$$\int_\Omega \hat{\boldsymbol{\sigma}}^s : \delta \mathbf{e}^s d\Omega = \langle \delta \mathbf{u}^s \rangle [\tilde{\mathbf{K}}] \{\mathbf{u^s}\}, \tag{2}$$

where $\hat{\boldsymbol{\sigma}}^s$ and $\mathbf{e^s}$ are the stress and respectively strain tensors of the skeleton.
Other Biot parameters, such as resistivity, dynamic tortuosity, porosity, viscous and thermal lengths together with foam frame density are vital for the establishment of the equivalent mass, volume coupling and equivalent kinetic and compression matrices.
In order to precisely determine the acoustic pressure level inside a car cabin cavity the correct definition of the above listed porous absorber properties is imperative. Most influential w.r.t the acoustic wave transfer function acquisition is the Young's modulus of the skeleton [12], according to the results of the conducted Morris sensitivity study [13, 14], as in Fig. 1.

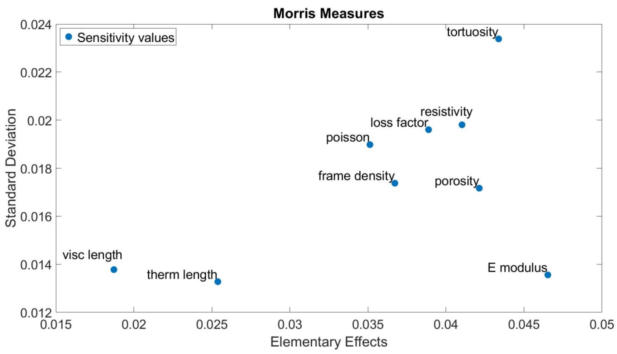

Figure 1. Morris analysis results w.r.t. Biot material parameters from [12].

Morris sensitivity methodology is an effective screening technique to identify most significant system parameters. It allows to calculate the so-called Elementary Effects of parameters to quantify the influence of each separate parameter on the target function with the help of finite differencing. Elementary Effects are depicted on the x-axis. The y-axis presents the standard deviation values as a measure of parameter interactions [14]. It can be seen in the Fig. 1 that the Young's modulus has indeed the highest Elementary Effect value and conveniently the lowest interaction with the rest of the group, making it an influential parameter.
Generally, the values of elastic parameters can be estimated by conducting dynamic experiments on spring-mass systems [15]. In laboratory conditions such systems get either excited with a shaker or with a loudspeaker and frequency response functions are measured by dividing the input signal on the bottom porous liner surface by the output signal on the upper surface of the liner [16, 17]. However, as simple as the concept of the measurement setup might seem, it poses a number of difficulties for precise parameter definitions. Among them are excitation plate-trim boundary condition influences, foam prestressing sensitivity and poor measurement reproducibility [18].
The current paper focuses on the development of a material parameter characterisation algorithm that circumvents the mentioned difficulties. In the following sections, first a set of experiments has been conducted to develop a reliable process to acquire measurement data for further material characterisation algorithms. In particular, the results of measurement campaigns to investigate the issues of measurement stability together with the effect of foam pre-stressing are presented. Afterwards the inverse optimization methodology to characterise porous absorber materials is discussed together with remarks on the structure-trim interface boundary conditions. Finally, the aspects of the uniqueness of the defined material parameter set are investigated and conclusions are drawn together with the outlook for further studies.

2. EXPERIMENTAL STUDIES

2.1 On stability of measurements

In the current work two types of PUR-foam samples with different viscous properties have been studied. Each liner was presented in several configurations: of 50x50x10 mm, 50x50x20 mm, 100x100x10 mm and 100x100x20 mm sizes respectively. The excitation was applied vertically by a shaker with a mounted excitation plate on top, as in Fig. 2.
Foam samples, glued to the excitation plate with a spray

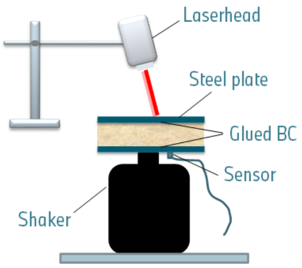

Figure 2. Measurement setup for transfer function evaluation.

glue, acted as a spring system and steel plates glued on top of them acted as a mass. The input signal was measured with an accelerometer attached to the excitation plate and the output signal was measured by a laser head, as in Fig. 2.

First of all, studies to investigate measurement stability were conducted. In reality, porous liners are applied in vehicles with a lighter elastic layer on top, which corresponds to a loading of 3-6 kg/m^2. As long as porous liners tend to involve inhomogeneities, certain pre-stressing is recommended to maintain measurement stability [18]. However, depending on stiffness characteristics of foams, samples can express high sensitivity to pre-loading and as a result, material parameter calculations can lead to overestimated stiffness values. To find an optimal loading value a series of measurements has been performed. Four corner points on the upper surface of the elastic layers were measured under pink noise excitation to determine deviation between the transfer function results for different locations. A measurement was considered stable, if four corresponding transfer functions brought coinciding curves.

A characteristic result of the measurements of 50x50x20 mm foam samples with a 1.6 mm thick magnesium plate on top is presented in Fig. 3. Such a plate creates a realistic pre-loading condition with 2.78 kg/m^2. It can be observed that the transfer function curves significantly deviate from each other, as the mass exhibited on the foam was not sufficient to stabilize the system. With a steel plate of 1.25 mm thickness, which corresponds to 9.8 kg/m^2 load, the results already show a better agreement between curves, but the amplitude values are still non-conforming, see Fig. 4.

Same measurements have been conducted for several samples of the same size. Steel plates of 1.25 mm, 1.5 mm, 1.8 mm, 2.0 mm, 2.65 mm, 3 mm and 4 mm and a magnesium plate of 1.6 mm have been glued on the top of the foam samples to investigate the pre-stressing influence on the measurement stability. First with the pre-loading condition of 20 kg/m^2 (2.65 mm thick steel plate) was an acceptable agreement achieved, see Fig. 5.

Similar results were obtained for the foam samples of 10 mm thickness with rare exceptions, where the steel plate thickness had to be increased up to 3-4 mm to eliminate the surface inhomogeneities. Mostly the four curves can be divided into two groups with similar damping values. This could happen because of the presence of bigger pores inside the samples on a specific side.

All in all, the higher the pre-loading, the more even is the signal distribution on the upper plate surface. However, in

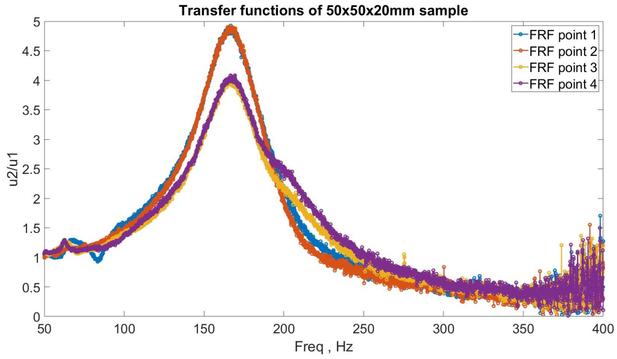

Figure 3. Laser measurement for 4 corner points on the magnesium 1.6 mm plate surface.

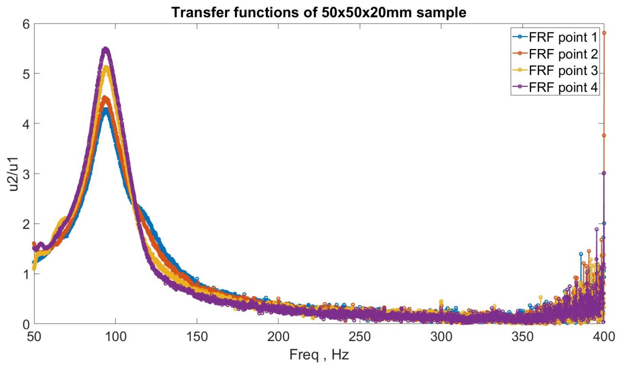

Figure 4. Laser measurement for 4 corner points on the steel 1.25 mm plate surface.

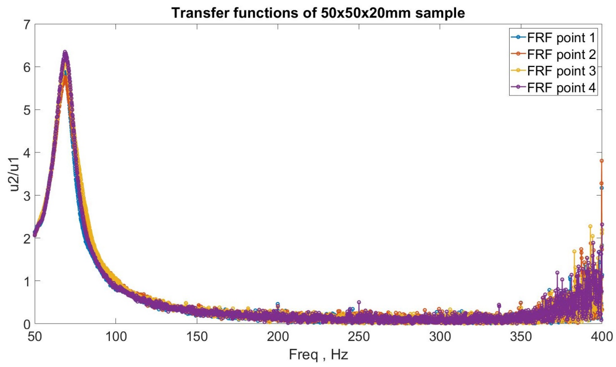

Figure 5. Laser measurement for 4 corner points on the steel 2.65 mm plate surface.

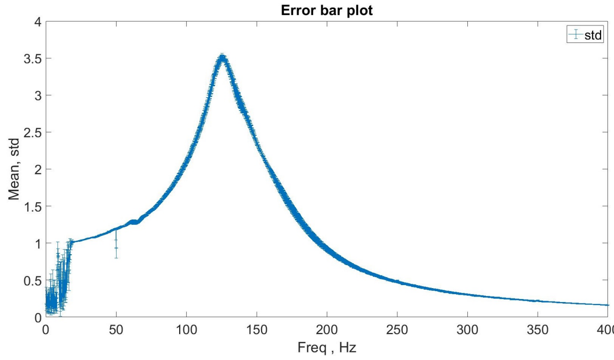

Figure 6. Error bar plot for samples of lower viscosity.

real life applications considerably lighter masses are used for conventional absorber elastic layers. Thus, massive plates can compress foam samples significantly and lead to exaggeratedly high foam stiffness value estimations. In this respect the pre-loading of 20-24 kg/m^2 was found to be optimal for further measurement campaigns (comprises 0.5% of the initial compression).

2.2 On measurement reproducibility

Porous absorbers are notoriously known for demonstrating poor measurement reproducibility [19, 20], which can compromise the validity of any related studies. In the current work samples of two PUR-foam types were investigated: absorbers with higher and lower viscosity. Generally, samples of lower viscosity performed considerably better in terms of measurement consistency and allowed for good reproducibility of test results. Five different samples of same size (50x50x10 mm) were cut from each type of liner. Mean transfer function values for each frequency in the range 0-400 Hz were calculated together with standard deviations of curve points from the mean value. A representative error bar plot for this type of samples can be observed in Fig. 6. Below around 20 Hz the results are noisy due to the measurement equipment precision. At 50 Hz a disturbance was detected as a result of the background radiation influence. The deviations from the mean value were acceptably low and the samples were further investigated for material characterisation purposes.
On the contrary, samples with high material viscosity values posed difficulties in terms of reproducibility and failed to provide satisfactory results, see Fig. 7. Highly viscous foams were not further used for characterisation studies.

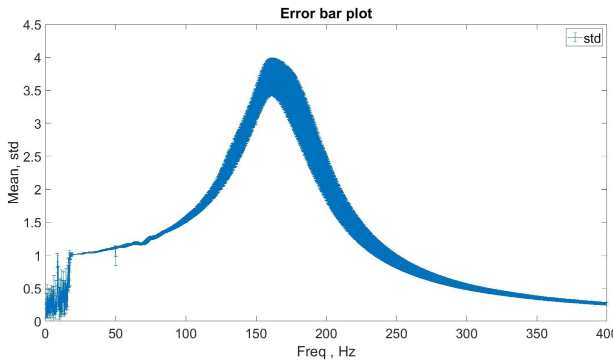

Figure 7. Error bar plot for samples of higher viscosity.

3. INVERSE OPTIMIZATION STUDIES

3.1 Genetic algorithms for Biot parameter definitions

Genetic algorithms (GAs) are optimization techniques inspired by the principles of natural evolution [21]. Demonstrating good performance even on complex optimization target functions, GAs can be applied for different applications in acoustics [21–23]. Several attempts have been made to characterise acoustic parameters of porous absorbers with the help of GAs [23, 24].
In the current paper inverse optimization techniques were applied to characterise not only acoustic Biot parameters,

but also structural parameters of the skeleton: Young's modulus, Poisson's ratio and loss factor. For the numeric calculations a custom program based on the Deal II library for finite element method (FEM) calculations was used. The program verification results showed perfect agreement with available reference solutions from [9]. The target function of the optimization was set to the root-mean-square (RMS) value of the sum of the differences between the measured and numerically calculated transfer function values for each frequency in the range of 50-400 Hz. Linear Lagrange polynoms were used as shape functions for the FEM calculations. For the measurements samples were glued on top of the shaker excitation plates. The numerical model was built as a coupled trim-elastic two-layered structure with a $1\ m/s$ excitation on the trim lower side. The optimization was performed using the genetic algorithms from the Standard Global Optimization Toolbox of Matlab. As thermal and viscous lengths were shown to have the smallest influence on the transfer functions in the explored frequency range (see Fig. 1), the values of these parameters were not subjected to optimization. 5 candidate solutions per variable were assigned, leading to the overall population size of 35. The maximum number of generations was set to 30.
As an example the results for the 50x50x10 mm samples are demonstrated in the current work. The corresponding convergence plot with mean and best values per generation can be observed in Fig. 8. Already after 5 generations the optimal parameter set was found. The resulting Biot values from the optimization can be seen in Tab. 1.

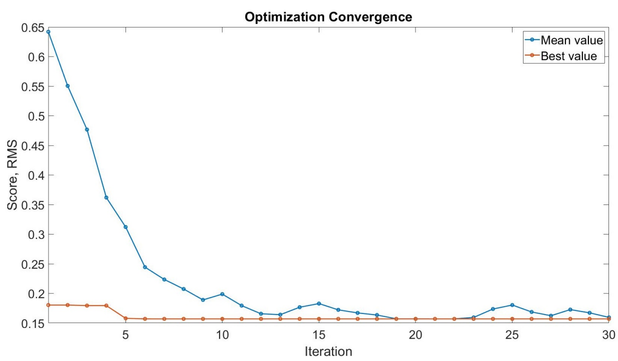

Figure 8. Convergence plot for the Biot parameter optimization.

As mentioned above, most influential parameters w.r.t. the transfer function values are the structural parameters of the skeleton. Unfortunately, comparing the optimization values of these parameters with measurement results directly is not possible, as long as measurement data only provides apparent parameter values instead of intrinsic ones [18]. One of the reasons is the effect of the boundary conditions of the sample on it's behavior. In particular, glued samples tend to perform considerably stiffer than in a freely laying state, see Fig. 9.

Table 1. Biot parameter results after genetic optimization.

Parameter	Optimized value	Unit
Air flow resistivity	37174	$N \cdot s/m^4$
Tortuosity	1.7504	–
Porosity	0.98	–
Frame density	66.08	kg/m^3
Young's modulus	88359	Pa
Poisson's ratio	0.2098	–
Loss factor	0.206	–

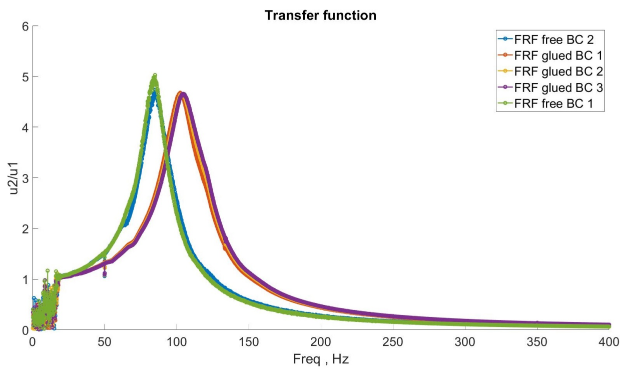

Figure 9. Influence of the boundary condition on the measurement results.

In the following subsection a structural parameter correction algorithm is presented to obtain realistic structural parameter values.

3.2 On the uniqueness of the solution

Generally, relying on one measurement result to obtain structural Biot parameter values in not sufficient, as long

as there could be several parameter configurations satisfying the same measurement. An incorrect set would fail to perform on a different liner configuration, eventually resulting in unusable material data.
There exist several updating techniques to correct structural parameter values. Among them are iterative methods with the help of FEM [25] and polynomial relations obtained for samples with different shape factors [26].
In the current research samples of sizes 100x100x10 mm and 100x100x20 mm were cut alongside with 50x50x10 mm and 50x50x20 mm samples. Further measurements on larger samples were conducted to receive transfer function values to introduce a second reference measurement for parameter update. For different Poisson's ratios between 0.1 and 0.48 corresponding Young's modulus and loss factor values were estimated with the help of quick two-parameter GA optimization studies. An exemplary result for the 50x50x20 mm sample can be seen in Tab. 2.

Table 2. Structural parameter sets for various Poisson's ratios.

Poisson's value -	Young's modulus *Pa*	Loss factor -
0.48	32500	0.195
0.45	42500	0.195
0.4	52000	0.19
0.337	63372	0.186
0.3	64000	0.19
0.2	71000	0.19
0.1	73236	0.19

The same parameter set was calculated for the larger samples of 100x100x20 mm, see Tab. 3. It can be observed that for higher Poisson's ratios the corresponding loss factor values for different sample configurations tended towards 0.195 with insignificant deviations starting from 0.43 for Poisson's ratio. The results for both samples were plotted against Poisson's ratio and Young's modulus values, as in Fig. 10.
It can be observed that the two curves for two corresponding samples crossed at (0.465;37000 Pa). These values are the corrected Poisson's ratio and the Young's modulus value for the 20 mm thick porous liner. Similar graphs were obtained for the material samples of 10 mm thickness, as in Fig. 11. The crossing point was (0.429; 43000 Pa). It should be mentioned that higher Poisson's ratio values are more common for such porous materials, making the updated parameter set more plausible in comparison to the initial inverse optimization characterisation set.

Table 3. Structural parameter sets for various Poisson's ratios.

Poisson's value -	Young's modulus *Pa*	Loss factor -
0.48	30000	0.195
0.45	44000	0.185
0.4	61000	0.175
0.337	76000	0.16
0.3	84000	0.158
0.2	96000	0.155
0.1	103000	0.147

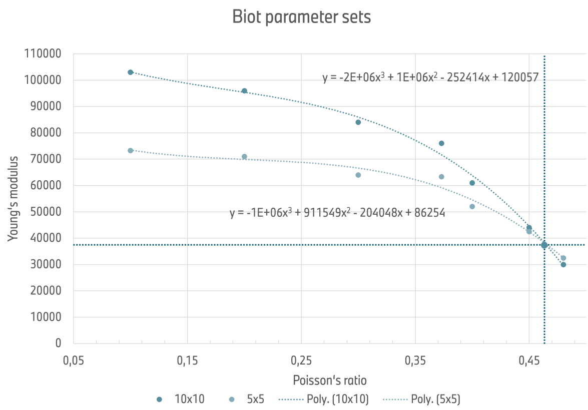

Figure 10. Structural parameter sets for samples of different shape factors.

4. CONCLUSION AND OUTLOOK

In the current paper an inverse Biot parameter characterisation approach was presented. The uniqueness of the solution was investigated and a structural parameter value correction algorithm was adapted. According to the conducted Morris sensitivity analysis results, acoustic parameters have a significantly lower influence on the transfer

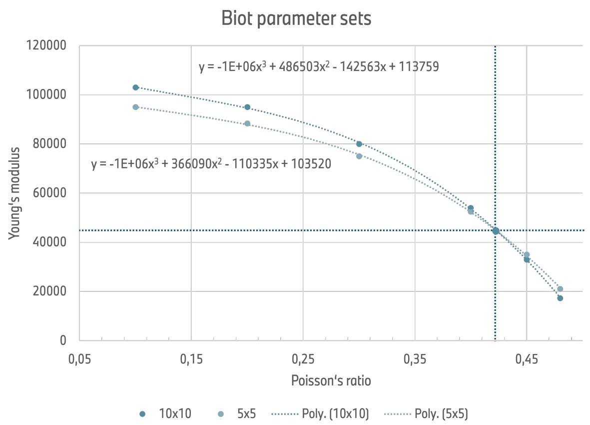

Figure 11. Structural parameter sets for samples of different shape factors.

function values in the targeted frequency range of 50-400 Hz (i.e. on the resonance frequency and the peak value). For this reason the focus was on structural Biot parameters, such as Young's modulus, Poisson's ratio and loss factor.

Moreover, the issues of measurement stability w.r.t the foam pre-stressing as well as of measurement reproducubility were studied. It was concluded that porous absorbers of lower viscosity demonstrated a smaller standard deviation from the mean measured transfer function values and thus delivered more reliable results.
Further investigations should be conducted to develop a strategy to measure liners with realistic heavy layer masses on top to exclude the restrictions imposed by heavier and stiffer plates on top of samples.

5. ACKNOWLEDGMENTS

Assistance provided by the Virtual Vehicle Research GmbH and the COMET K2 Program "K2 Digital Mobility" in the context of mutual collaboration is greatly appreciated. It vastly helped to establish the foundation for the current research and for the upcoming investigations. We thank our colleagues for constant support and valuable contributions.

6. REFERENCES

[1] M. J. M. Nor, M. H. Fouladi, H. Nahvi, and A. K. Ariffin, "Index for vehicle acoustical comfort inside a passenger car," *Applied Acoustics*, vol. 69, pp. 343–353, 2008.

[2] Z. Liu, M. Fard, and J. L. Davy, "Prediction of the acoustic effect of an interior trim porous material inside a rigid-walled car air cavity model," *Applied Acoustics*, vol. 165, p. 107325, 2020.

[3] Z. Liu, M. Fard, and J. Davy, "Acoustic properties of the porous material in a car cabin model," in *Twenty-Third International Congress on Sound and Vibration*, pp. 1–8, International Institute of Acoustics and Vibration, 2016.

[4] S. Ahsani, C. Claeys, T. Zielinski, Jankowski, F. Scarpa, W. Desmet, and E. Deckers, "Sound absorption enhancement in poro-elastic materials in the viscous regime using a mass–spring effect," *Journal of Sound and Vibration*, vol. 511, p. 116353, 2021.

[5] M. A. Biot, "Theory of propagation of elastic waves in a fluid-saturated porous solid. i. low-frequency range," *The Journal of the Acoustical Society of America*, vol. 28, no. 2, pp. 168–178, 1956.

[6] M. A. Biot, "Theory of propagation of elastic waves in a fluid-saturated porous solid. ii. higher frequency range," *The Journal of the Acoustical Society of America*, vol. 28, no. 2, pp. 179–191, 1956.

[7] M. A. Biot, "Generalized theory of acoustic propagation in porous dissipative media," *The Journal of the Acoustical Society of America*, vol. 34, no. 9A, pp. 1254–1264, 1962.

[8] J. Allard and N. Atalla, *Propagation of sound in porous media: modelling sound absorbing materials 2e*. John Wiley & Sons, 2009.

[9] N. Atalla, R. Panneton, and P. Debergue, "A mixed displacement-pressure formulation for poroelastic materials," *The Journal of the Acoustical Society of America*, vol. 104, no. 3, pp. 1444–1452, 1998.

[10] N. Atalla, M. A. Hamdi, and R. Panneton, "Enhanced weak integral formulation for the mixed (u_{-}, p_{-}) poroelastic equations," *The Journal of the Acoustical Society of America*, vol. 109, no. 6, pp. 3065–3068, 2001.

[11] Y. J. Kang and J. S. Bolton, "Finite element modeling of isotropic elastic porous materials coupled with acoustical finite elements," *The Journal of the Acoustical Society of America*, vol. 98, no. 1, pp. 635–643, 1995.

[12] M. Bronzova, A. Bocquillet, and M. Schanz, "New porous absorber simulation techniques in the context of finite element modelling," in *Noise and Vibration: Emerging Methods, NOVEM 2023, Auckland, New Zealand, January 10-12, 2023. Proceedings (submitted)*, Institute of Noise Control Engineering of the USA Digital Library, 2023.

[13] F. Campolongo, J. Cariboni, and A. Saltelli, "An effective screening design for sensitivity analysis of large models," *Environmental Modelling & Software*, vol. 22, no. 10, pp. 1509–1518, 2007.

[14] L. Paleari, E. Movedi, M. Zoli, A. Burato, I. Cecconi, J. Errahouly, E. Pecollo, C. Sorvillo, and R. Confalonieri, "Sensitivity analysis using morris: Just screening or an effective ranking method?," *Ecological Modelling*, vol. 455, p. 109648, 2021.

[15] M. Nortemann, *Characterisation of Young's Modulus and Loss Factor of Damping Materials*. PhD thesis, Nelson Mandela Metropolitan University, 2014.

[16] C. G. Albert, G. Veronesi, E. Nijman, and J. Rejlek, "Prediction of the vibro-acoustic response of a structure-liner-fluid system based on a patch transfer function approach and direct experimental subsystem characterisation," *Applied Acoustics*, vol. 112, pp. 14–24, 2016.

[17] J. Rejlek, E. Nijman, G. Veronesi, and C. Albert, "A patch transfer function approach for combined computational-experimental analysis of vibro-porous-acoustic problems," *Automotive NVH Technology*, pp. 99–117, 2016.

[18] F. Chevillotte, F. Ronzio, C. Bertolini, M. T. Hoang, *et al.*, "Inter-laboratory characterization of biot parameters of poro-elastic materials for automotive applications," tech. rep., 2020.

[19] P. Bonfiglio, F. Pompoli, K. V. Horoshenkov, M. I. B. S. A. Rahim, L. Jaouen, J. Rodenas, *et al.*, "How reproducible are methods to measure the dynamic viscoelastic properties of poroelastic media?," *Journal of Sound and Vibration*, vol. 428, pp. 26–43, 2018.

[20] F. Pompoli, P. Bonfiglio, K. V. Horoshenkov, A. Khan, L. Jaouen, F.-X. Bécot, *et al.*, "How reproducible is the acoustical characterization of porous media?," *The Journal of the Acoustical Society of America*, vol. 141, no. 2, pp. 945–955, 2017.

[21] V. Romero-García, E. Fuster-García, J. V. Sánchez-Pérez, L. M. Garcia-Raffi, X. Blasco, J. Herrero, and J. Sanchis, "Genetic algorithm in the optimization of the acoustic attenuation systems," in *Computational and Ambient Intelligence: 9th International Work-Conference on Artificial Neural Networks, IWANN 2007, San Sebastián, Spain, June 20-22, 2007. Proceedings 9*, pp. 614–621, Springer, 2007.

[22] M. Baulac, J. Defrance, and P. Jean, "Optimisation with genetic algorithm of the acoustic performance of t-shaped noise barriers with a reactive top surface," *Applied Acoustics*, vol. 69, no. 4, pp. 332–342, 2008.

[23] X. Xu and P. Lin, "Parameter identification of sound absorption model of porous materials based on modified particle swarm optimization algorithm," *PloS One*, vol. 16, no. 5, p. e0250950, 2021.

[24] P. Shravage, S. Jain, and N. Karanth, "A comparison of analytical and optimization inverse techniques for characterizing intrinsic parameters of porous materials," in *INTER-NOISE and NOISE-CON Congress and Conference Proceedings*, vol. 2010, pp. 1346–1355, Institute of Noise Control Engineering, 2010.

[25] S. Sim and K.-J. Kim, "A method to determine the complex modulus and poisson's ratio of viscoelastic materials for fem applications," *Journal of Sound and Vibration*, vol. 141, no. 1, pp. 71–82, 1990.

[26] C. Langlois, R. Panneton, and N. Atalla, "Polynomial relations for quasi-static mechanical characterization of isotropic poroelastic materials," *The Journal of the Acoustical Society of America*, vol. 110, no. 6, pp. 3032–3040, 2001.